# 25°C and 1 atm dissolution experiments of sepiolite and kerolite

R. K. STOESSELL

Department of Geology and Geophysics, University of New Orleans, New Orleans, LA 70148, U.S.A.

Abstract—Fine-grained sepiolite ($Mg_2Si_3O_{7.5}(OH) \cdot 3H_2O$) and kerolite ($Mg_3Si_4O_{10}(OH)_2 \cdot H_2O$) samples from lacustrine-playa sediments at Amboseli, Kenya, were used in dissolution experiments with five different solutions at 25°C for time periods approaching 10 years. The hydrolysis reactions

$$\text{sepiolite} + 4H^+ = 2Mg^{2+} + 3SiO_2(aq) + 5.5H_2O$$

$$\text{kerolite} + 6H^+ = 3Mg^{2+} + 4SiO_2(aq) + 5H_2O$$
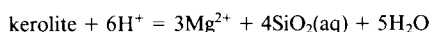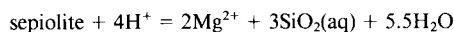
have estimated log K values of 15.76 ± 0.18 and 25.79 ± 0.24, respectively (error estimate 1 s.d.). The estimate for kerolite hydrolysis is a minimum value due to the possibility of kerolite beginning to transform to a more stable phase during the experiments. The corresponding values of the $\Delta \bar{G}^0_{sep}$ and $\Delta \bar{G}^0_{ker}$ are $-4,624,340$ and $-5,736,700$ J mol^{-1}, respectively, relative to the data sources in the text. These values replace preliminary results reported earlier after approximately one year of dissolution time in the experiments. The sepiolite log K is in good agreement with the value of 15.86 predicted by CHRIST et al. (Amer. J. Sci., 1973) from measurements at higher temperatures.

Under earth-surface conditions, kerolite is metastable with respect to sepiolite in solutions at equilibrium or super-saturated with respect to quartz. However, the solubility difference is minor, suggesting that reaction kinetics exert a major control in determining which mineral forms in the sedimentary environment.

INTRODUCTION

AUTHIGENIC MAGNESIUM SILICATES are predicted from thermodynamic stabilities but are uncommon in near-surface environments. Sepiolite ($Mg_2Si_3O_{7.5}(OH) \cdot 3H_2O$) is a minor exception, because it is occasionally found in deep sea sediments (HATHAWAY and SACHS, 1965), in playa and lacustrine sediments (BRADLEY, 1930; PARRY and REEVES, 1968; PAPKE, 1972; STOESSELL and HAY, 1978; KHOURY et al., 1982), and in soils (VANDEN HEUVEL, 1966). The reported occurrences of sepiolite decrease with an increase in age of the associated sediments (GRIM, 1968, p. 554).

Kerolite ($Mg_3Si_4O_{10}(OH)_2 \cdot nH_2O$, with $n \simeq 1$ for H_2O^+ water) is an uncommon mineral, formerly thought to be a mixture of stevensite and serpentine but is actually a hydrated and disordered talc-like mineral (BRINDLEY et al., 1977). Authigenic kerolite has been reported in lacustrine-playa sediments at Amboseli, Kenya (STOESSELL and HAY, 1978; HAY and STOESSELL, 1984), at Amargosa Desert, Nevada (KHOURY et al., 1982; EBERL et al., 1982), and at Stewart Springs, California (JONES, 1986). Nickel-rich kerolites are occasionally associated with nickel deposits in laterites, e.g., at Goles Mountain, Yugoslavia (MAKSIMOVIC, 1966). In a fine-grained mixture of clays, the approximate 10 Å basal spacing of kerolite is easily confused with illite in an X-ray diffraction pattern. For this reason kerolite may often be overlooked in sediments.

The present study was made to evaluate the thermodynamic stabilities of sepiolite and kerolite at 25°C and 1 atm, and to provide estimates of thermodynamic parameters needed to evaluate the stability fields of the two minerals during diagenesis. The previous experimental results for sepiolite disagree by 16.7 kJ mol^{-1} in the standard state free energy of formation at 25°C (WOLLAST et al., 1968; CHRIST et al., 1973). A literature search failed to locate any previous experimental studies on kerolite.

Dissolution reactions were run in different solutions at 25°C and 1 atm for time periods approaching ten years. Similar activity quotients for the final solution measurements in different solutions suggest equilibrium conditions were reached or closely approached. For the normal range of $SiO_2(aq)$ concentrations in natural waters, kerolite was found to be metastable with respect to sepiolite. However, the difference in solubility is small. The results for sepiolite from this study are in good agreement with those predicted by CHRIST et al. (1973) from dissolution measurements at higher temperatures. The metastability of kerolite relative to sepiolite has been previously suggested (among others) by JONES (1986) on the basis of field studies.

Standard state thermodynamic parameters at 25°C and 1 bar for sepiolite were computed from data in this study or estimated using algorithms including a structural analogue involving talc, brucite, "zeolitic" water, and Mg-hydrated water. These parameters are consistent with two of the three experimental measurements of CHRIST et al. (1973) at higher temperatures. Their measurement at 70°C appears inconsistent with our 25°C measurement and their own measurements at 51° and 90°C.

PREVIOUS EXPERIMENTAL WORK

The precipitation of poorly-crystalline sepiolite at room temperature has been reported in several studies (SIFFERT, 1962; WOLLAST et al., 1968; COUTURE, 1977). WOLLAST et al. (1968) precipitated a magnesium silicate from sea water containing aqueous SiO_2 additions of 26 to 140 ppm. The identification of sepiolite was based on a partial wet chemical analysis, an infrared absorption spectrum, and electron micrographs of the precipitate. Their X-ray powder diffraction pattern lacked the diagnostic 12 Å peak. They reported an average log activity product of 18.78 for the hydrolysis of sepiolite in reaction (1).

$$Mg_2Si_3O_{7.5}(OH) \cdot 3H_2O + 4H^+ = 2Mg^{2+}$$

$$+ 3SiO_2(aq) + 5.5H_2O \quad (1)$$
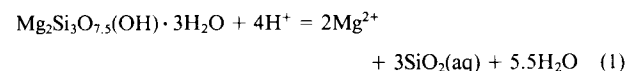
CHRIST et al. (1973) reported solution equilibration data with a well-crystallized natural sepiolite at 51°, 70°, and 90°C. Their estimate of the log equilibrium constant at 25°C for reaction (1) was 15.86, as recalculated from their reported value of -40.1 for the log activity product of $(a^2_{Mg^{2+}} a^3_{H_4SiO_4} a^4_{OH^-})$. They also demonstrated a greater solubility at 51°C for a poorly-crystallized sepiolite than a well-crystallized sepiolite and suggested this effect was a partial explanation for the larger solubility reported by WOLLAST et al. (1968). The increased solubility with decreasing crystallinity was less significant at higher temperatures.

No previous experimental work on kerolite stabilities have been found in the literature. Log activity product values in this study will be for the kerolite hydrolysis reaction given below.

$$Mg_3Si_4O_{10}(OH)_2 \cdot H_2O + 6H^+ = 3Mg^{2+} + 4SiO_2(aq) + 5H_2O \quad (2)$$
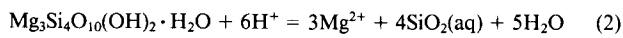
PROCEDURES AND EXPERIMENTAL RESULTS

Description of samples and experimental and analytical methods

The samples of sepiolite and kerolite used in the experiments were collected at Amboseli, Kenya (STOESSELL, 1977). These minerals formed in a lacustrine-playa environment and are massive and ex-

tremely fine-grained. The sepiolite is a white, porous, chalky material, and the kerolite is a waxy, gray clay having conchoidal fracture. Secondary electron photomicrographs, Figs. 1a and 1b, show the characteristic fibrous nature of the sepiolite surface and the crinkly and flaky or "smectitic looking" kerolite surface.

X-ray diffraction patterns, optical examination, and scanning electron microscopy were used to check for impurities. None were found for the sepiolite; however, upon glycolation, the kerolite had a minor expandable smectite component, presumably saponite, showing on the X-ray diffraction pattern of oriented samples. The presence of this impurity will affect the results of the kerolite dissolution experiments if the solutions equilibrated with the impurity. In this study, a consistent set of measured kerolite hydrolysis products from the different experiments (described below) was used as an indication that the solution compositions were controlled by dissolution of kerolite.

Tables 1 and 2 contain diagnostic data of the samples together with the available appropriate data from the literature for comparison. Wet chemical analyses are reported in Table 1, and the X-ray powder diffraction d spacings along with the refined lattice constants for sepiolite are listed in Table 2. The minerals are nearly pure hydrated magnesium silicates. Although, not shown here, the infrared absorption spectra of the samples were reported by STOESSELL (1977, p.
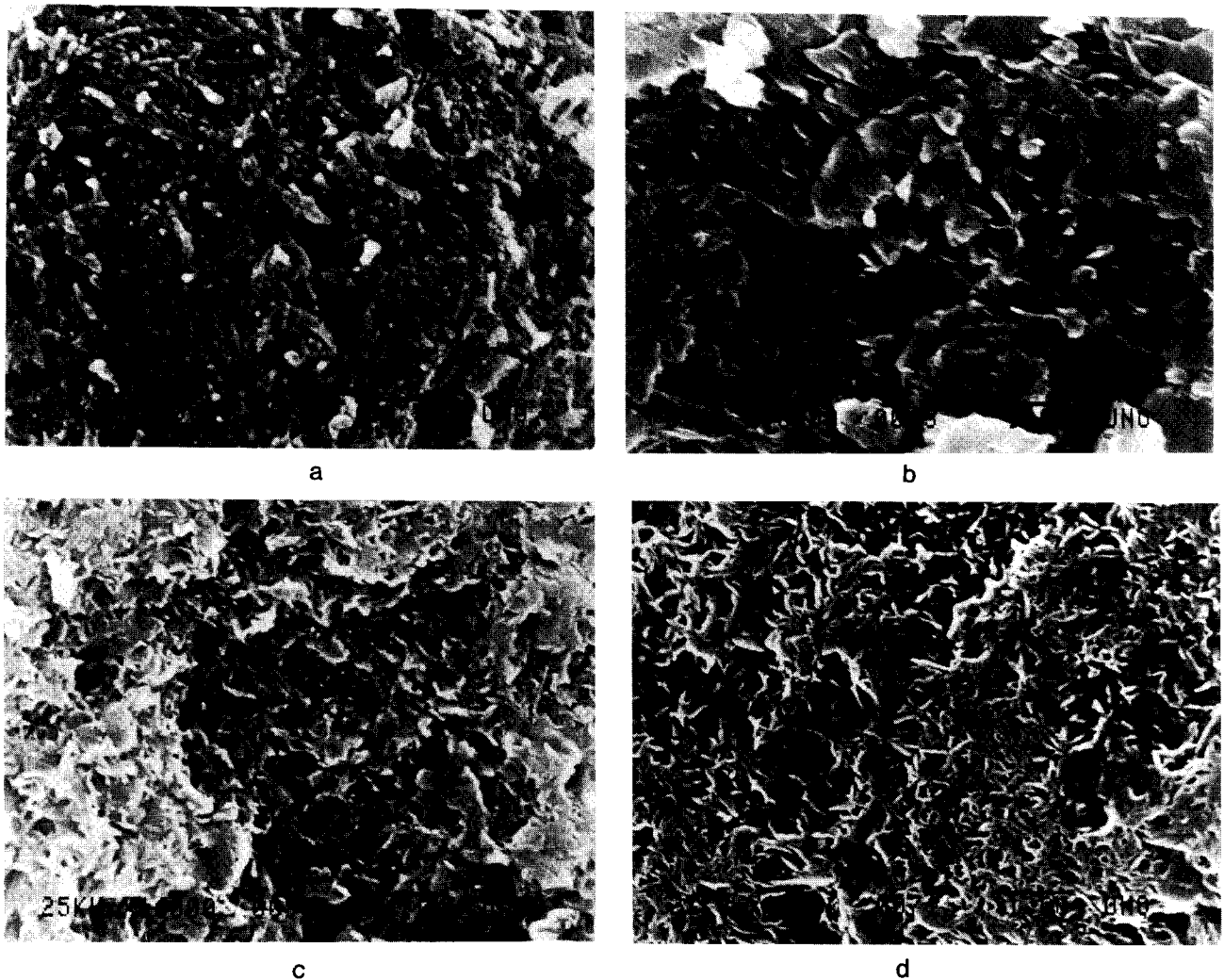
FIG. 1. Secondary electron photomicrographs of unreacted sepiolite and kerolite grains, (1a) and (1b), respectively, and typical photomicrographs of reacted kerolite grains, (1c) and (1d), respectively, from material in Exps. 9 and 7. Scale is 1.6 cm per μm. Photomicrographs of reacted sepiolite grains (not shown) were identical to unreacted sepiolite grains.

Table 1. Chemical analyses of sepiolite and kerolite samples.*

wt. %	1	2**	3	4	5**	6	7
SiO_2	55.65	53.70	54.83	60.49	54.51	58.73	58.33
TiO_2		0.12	n.r.		0.03	0.03	n.r.
Al_2O_3		1.15	0.28		0.49	0.53	0.09
Fe_2O_3		0.64	0.45		0.10	0.11	0.53
FeO		0.02	n.r.				n.r.
MnO		0.004	n.r.		0.000	0.000	n.r.
NiO		0.000	n.r.		0.000	0.000	0.27
MgO	24.89	23.31	24.51	30.44	28.01	30.18	32.02
CaO		0.03	0.55		0.52	0.56	0.14
Na_2O		0.67	0.03		0.85	0.92	0.00
K_2O		0.61	0.35		0.26	0.28	0.04
P_2O_5		0.02	n.r.		0.03	0.03	n.r.
H_2O+	19.46	9.83	10.74	9.07	7.97	8.58	8.50
H_2O^-		9.76	8.18	***	7.18	***	***
Total	100.00	99.86	99.92	100.00	99.95	99.95	99.92
molar							
Mg/Si	0.67	0.65	0.67	0.75	0.77	0.77	0.82

1. Sepiolite, based on ideal formula, $Mg_2Si_3O_{7.5}(OH)\cdot 3H_2O$. 2. Sepiolite, Amboseli, Kenya. 3. Sepiolite, Yavapai County, Arizona (Kaufman, 1943). 4. Kerolite, based on ideal formula, $Mg_3Si_4O_{10}(OH)_2\cdot H_2O$ (with H_2O^- = 0). 5. Kerolite (gray) Amboseli, Kenya. 6. Recalculation of 5 with H_2O^- = 0. 7. Kerolite, Madion County, North Carolina (Brindley et al., 1977, sample #481.90).
* The analyses of the Amboseli samples were made by Stoessell (1977) using a modified procedure of Shapiro and Brannock (1962). Standard deviations from dublicate analyses of 3 kerolites and 3 sepiolites were SiO_2 ± 0.09, TiO_2 ± 0.01, Al_2O_3 ± 0.04, Fe_2O_3 (total Fe) ± 0.02, MgO ± 0.05, CaO ± 0.02, Na_2O ± 0.02, K_2O ± 0.03.
** Samples used in experiments in this study.
*** Analysis computed with H_2O^- = 0.

55). The dehydration trends are shown in Fig. 2 for the samples. Both sepiolite and kerolite have appreciable H_2O^- water. In this study, this water is included for sepiolite but not for kerolite in computing its standard state thermodynamic properties, following the conventions used with zeolites and smectites, respectively.

The water in the gray kerolite ($Mg_3Si_4O_{10}(OH)_2\cdot nH_2O$) can be estimated from analysis #6 in Table 1. Neglecting H_2O^- water and assuming 11 oxygen atoms to balance all cations except hydrogen, results in a value of 0.92 for n. BRINDLEY et al. (1977) reported n ranges between 0.8 and 1.2 for kerolites, neglecting H_2O^- water. The ideal value of one was used in this study in computing the standard state free energy of formation of kerolite from the average experi-

mentally-measured hydrolysis constant. The values of the hydrolysis constant were not significantly affected by the value of n, because the activity of water approached unity in the dilute solutions used in the experiments.

Prior to the beginning of the experiments, the samples were broken into small pieces, ground in a mortar, sieved, washed overnight in distilled and deionized water and then dried. The grain size used in the sepiolite experiments was between 63 and 124 microns and in the kerolite experiments, between 41 and 63 microns.

Ten dissolution experiments, each involving 1 gram of sample reacting with 400 ml of solution, were run at 25°C and 1 atm in 500 ml polyethylene bottles. Sepiolite was the reactant mineral in Exps.

Table 2. X-ray powder data for sepiolite and kerolite.

	sepiolite				kerolite*			
Brindley (1959)		Amboseli	sample**		Brindley et al. (1977)		Amboseli	sample
hkl	d (calc.) Å	d Å	I		hkl	d Å	d Å	I
110	12.07	12.11	(100)		001	9.8 to 10.1	10.3	(100)
130	7.48	7.66	(5)				4.56	(75)
200	6.750	6.73	(5)		003	3.2	3.18	(50)
040	6.742						2.57	(55)
060	4.495	4.495	(15)				1.526	(55)
131	4.301	4.332	(15)					
260	3.741	3.754	(15)					
080	3.370	3.339	(20)					
112,371	2.560	2.563	(20)					
		1.529	(5)					

* Calculated d spacings are not presented because the unit cell and space group of kerolite are not known.
** Lattice constants computed from a least squares refinement for the Amboseli sepiolite are a = 13.53 ± 0.07, b = 26.89 ± 0.06, and c = 5.33 ± 0.03 Å.
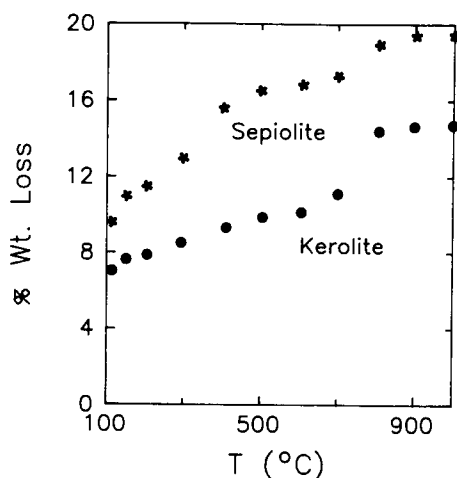
FIG. 2. Dehydration curves of sepiolite and kerolite samples used in this study. Dehydration was determined using successive 24 hour heating periods in an oven at 110°, 150°, 200°, and at 100° intervals to 1000°C.

1 through 5 and kerolite, in Exps. 6 through 10. Experiments 1 through 5 were run for almost 10 years and Exps. 6 through 10 for nearly 9.5 years. The initial solution compositions were:

Exps. 1 and 6—distilled-deionized water,
Exps. 2 and 7—0.0012 molal HCl,
Exps. 3 and 8—0.0024 molal HCl,
Exps. 4 and 9—0.0010 molal Na_2CO_3, and
Exps. 5 and 10—0.0100 molal Na_2CO_3.

Reagent grade HCl solutions and Na_2CO_3 salt were used to make the initial solutions. Duplicates of each experiment were begun to allow for the sampling procedure described below.

The first 13 months of Exps. 1-5 and 6 months of Exps. 6-10 correspond to the initial stage of the experiments. The reaction bottles were left open to the atmosphere to equilibrate with CO_2 and shaken once a day. Distilled water was added to compensate that lost by evaporation. For the remainder of the reaction time the bottles were kept closed, allowing for slower exchange of gases with the atmosphere. In addition, the periodic shaking was reduced to once or twice a month. During the final two years of reaction, the bottles were stored in a constant-temperature GCA/Precision refrigerator through which air circulated at 25° ± 1°C. At all other times, the bottles were stored in rooms in which the temperature fluctuated ±2° from 25°C.

The bottles were sampled at regular time intervals during the initial stage described above and then at the end of the experiments. A sample set corresponds to five samples taken at the same time from either the five sepiolite experiments or kerolite experiments. During the initial stage (described above), eleven sample sets and 8 sample sets, respectively, were taken from the sepiolite and kerolite experiments. The sampling procedure for sample sets 1-10 for Exps. 1-5 and sample sets 1-7 for Exps. 6-10 began with shaking each bottle and waiting for half an hour while the sediment settled. Approximately 35 ml of "clear" solution were then withdrawn. Five ml of this solution were used in an alkalinity titration to a pH of 4.5 and the remainder filtered through a Whatman #42 filter. Each reaction bottle was then reshaken and the pH read directly in the bottle using a combination Beckman #39030 pH electrode with a Corning Model 10 pH meter. The pH meter and electrode were calibrated with pH buffer solutions of 7.00 and 10.00 between each reading. Solutions from the duplicate bottles were then added to replace fluids taken in sampling. During the first month of an experiment the solution taken from each duplicate bottle was replaced with the original starting solution, afterwards the solution was replaced with distilled-deionized water.

The sampling procedure for sample set 11 in Exps. 1-5 and sample set 8 in Exps. 6-10 was similar to that described above except that distilled-deionized water was added to replace the fluid removed during sampling. The procedure for the final sample sets, #12 of Exps.

1-5 and #9 of Exps. 6-10, included measuring the pH directly in the bottle prior to withdrawing the fluid and measuring the alkalinity on the filtered samples. In addition, sample 9 from Exp. 10 was filtered through a 0.45 micron filter to remove a suspension of very fine material.

The filtered fluids were used to analyze for SiO_2 and the major cations. Non-polymerized SiO_2 concentrations were determined with the molybdate blue method (MULLIN and RILEY, 1955) and total Ca, Mg, Na, and K concentrations were measured by atomic absorption spectroscopy. For all but the final samples, 1000 ppm lanthanum were added to suppress silica interference for Ca and Mg and to reduce ionization of Na and K. For the final samples, 1000 ppm Sr were used to suppress silica interference and 1000 ppm K and 1000 ppm Na were added to reduce ionization of Na and K, respectively.

The solid materials in the experiments were examined by X-ray diffraction at the conclusion of the experiments. The patterns were identical to those made at the beginning of the experiments, implying that if new phases precipitated, they were below the detection limit. Examination of the surface of the reacted solids by scanning electron microscopy did not show any new phases. The surface of the reacted sepiolite grains had the same fibrous texture as the unreacted grain shown in Fig. 1a. The surface of the reacted kerolite grains still appeared crinkly or "smectitic looking" as in Fig. 1b. However, the edges of the plates making up the crinkly surface were typically raised and often looked frayed (Figs. 1c, d), implying kerolite may have been beginning to dissolve and transform by back-precipitation to a more stable phase such as sepiolite.

Experimental results

The log activity product (Q) for reactions (1) and (2) are

$$\log Q_{sep} = 2 \log \frac{a_{Mg^{2+}}}{(a_{H^+})^2} + 3 \log a_{SiO_2(aq)} + 5.5 \log a_{H_2O} \quad (3)$$

and

$$\log Q_{ker} = 3 \log \frac{a_{Mg^{2+}}}{(a_{H^+})^2} + 4 \log a_{SiO_2(aq)} + 5 \log a_{H_2O} \quad (4)$$

where a represents activity. The activities of the solid phases were unity and those of water approached unity in the experiments.

The entire set of analytical data for the experiments are to be found in the Appendix. The final sample sets, #12 from Exps. 1-5 and #9 from Exps. 6-10 represent approximately ten years of reaction and were used to estimate conditions of equilibrium for the mineral hydrolysis reactions. As discussed previously, the earlier sample sets were taken during the first 13 and 6 months, respectively, of the sepiolite and kerolite experiments. Their reaction time periods are not significant relative to those of the final sample sets and were not used to estimate equilibrium conditions.

The values of the computed log Q_{sep} and log Q_{ker} are listed for the entire set of samples taken in all the experiments and are included in the Appendix. The "Q" values were calculated using REACT, an unpublished computer program written by Stoessell. Activities were obtained by distributing the measured total concentrations among the known aqueous species assuming thermodynamic equilibrium. In this distribution, the extended Debye-Hückle equation (HELGESON et al., 1981, Eqn. 298) was used to calculate aqueous activity coefficients of charged species. The activity coefficient of neutral species was assigned to that of dissolved CO_2 (HELGESON, 1969), and the method of LIETZKE and STOUGHTON (1975) was used to predict the activity coefficient of water. The equilibrium constants of the aqueous dissocia-

tion reactions and the CO_2 (gas) hydrolysis reaction at 25°C and their sources are listed in Table 3.

REACT utilizes a nonlinear mass balance equation for each aqueous thermodynamic component in which the appropriate aqueous complexes are included through the dissociation reactions. The set of equations are solved simultaneously for the concentration of each thermodynamic component using a Newton-Raphson procedure to linearize the equations and iterate to reach convergence (as described by REED, 1982). At each iteration, the resulting matrix is solved by maximum pivot strategy applied to a Gauss-Jordan elimination.

Inorganic carbon was determined by varying the inorganic carbon input into *REACT* until the predicted alkalinity matched the measured alkalinity. Because Cl concentrations were not measured, they were either computed within the iteration sequence of *REACT* using electrical neutrality or, in Exps. 4–5 and 9–10, the concentration was assumed to have originated from KCl leakage of the combination pH-reference electrode.

Errors in the equilibrium constants of the dissociation reactions will produce the largest error in the computed log Q values in samples from Exps. 5 and 10. These experiments had the highest pH values and highest inorganic carbon concentrations. In the final samples of these experiments, the $MgCO_3^0$ and $H_3SiO_4^-$ complexes accounted for approximately 30% of the total Mg and SiO_2 concentrations.

The aqueous molal Mg:SiO₂ ratio *versus* log reaction time in seconds is plotted for the sepiolite experiments on Fig. 3 and for the kerolite experiments on Fig. 4. This ratio should be 0.67 for the congruent dissolution of sepiolite and 0.75 for that of kerolite. Initially, for both sepiolite and kerolite experiments, the Mg concentrations in the hydrolysis reactions begun in acidic solutions were too high and in basic solutions, too low. This was a result of H^+ exchange with
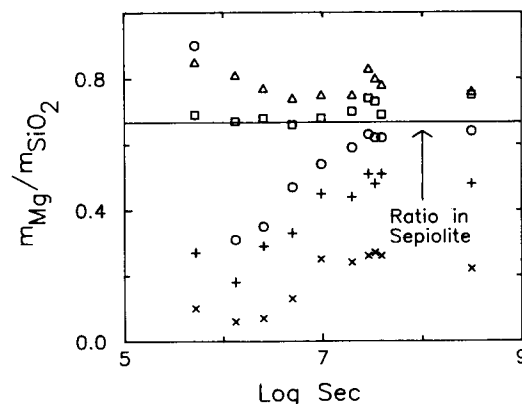

FIG. 3. Aqueous molal ratios of Mg:SiO₂ as a function of reaction time during sepiolite hydrolysis in Exp. 1, O; Exp. 2, □; Exp. 3, △; Exp. 4, +; and Exp. 5, ×.

Mg^{2+} in acidic solutions, and perhaps reflects the formation of brucite surface layers in basic solutions.

The aqueous molal Mg:SiO₂ ratios in the kerolite experiments were close to 0.75 after several months of reaction. At the end of the experiments, only the dissolution reaction begun in the most basic solution (Exp. 10) appeared to be incongruent. The aqueous molal Mg:SiO₂ ratios in the sepiolite experiments took longer to approach that expected for congruent dissolution. At the end of the experiments, both of the dissolution reactions begun in basic solutions remained incongruent. For comparison purposes, sepiolite dissolution in the experiments of CHRIST *et al.* (1973) approached congruency at 51°C but was incongruent at 70° and 90°C.

For sample sets 1–11 of Exps. 1–5 and sample sets 1–8 of Exps. 6–10, the log Q_{sep} and log Q_{ker} values (see Appendix), respectively, showed significant variation for samples representing equal amounts of reaction time. Presumably these differences reflect insufficient reaction time (on the order of a year) to reach equilibrium. However, the final log Q values, listed in the Appendix tables (marked with *) and representing nearly 10 years of reaction time, show only minor variation. The average log Q_{sep} and log Q_{ker} values were 15.76 (±0.18

Table 3. 25°C and 1 atm log K values for aqueous dissociation reactions and CO_2 gas hydrolysis.

Reaction	log K	source
1) $H^+ + OH^- = H_2O$	13.99	(a)
2) $HCl^° = H^+ + Cl^-$	6.10	(b)
3) $HCO_3^- = H^+ + CO_3^{2-}$	-10.33	(c)
4) $H_2CO_3^° = 2H^+ + CO_3^{2-}$	-16.68	(c)
5) CO_2 gas $+ H_2O = 2H^+ + CO_3^{2-}$	-18.15	(c)
6) $H_2SiO_4^{2-} + 2H^+ = SiO_2$ aq $+ 2H_2O$	21.32	(d)
7) $H_3SiO_4^- + H^+ = SiO_2$ aq $+ 2H_2O$	9.69	(e)
8) $Ca(OH)^+ + H^+ = Ca^{2+} + H_2O$	12.60	(f)
9) $CaHCO_3^+ = Ca^{2+} + H^+ + CO_3^{2-}$	-11.43	(c)
10) $CaCO_3^° = Ca^{2+} + CO_3^{2-}$	-3.22	(c)
11) $Mg(OH)^+ + H^+ = Mg^{2+} + H_2O$	11.79	(g)
12) $MgHCO_3^+ = Mg^{2+} + H^+ + CO_3^{2-}$	-11.41	(h)
13) $MgCO_3^° = Mg^{2+} + CO_3^{2-}$	-2.98	(i)
14) $KCl^° = K^+ + Cl^-$	1.41	(j)
15) $NaOH^° + H^+ = Na^+ + H_2O$	14.70	(k)
16) $NaCl^° = Na^+ + Cl^-$	0.93	(a)
17) $NaCO_3^- = Na^+ + CO_3^{2-}$	-0.96	(f)
18) $NaHCO_3^° = Na^+ + H^+ + CO_3^{2-}$	-10.07	(f)

(a) Helgeson et al. (1974, 1981); (b) Robinson (1936); (c) Plummer and Busenberg (1982); (d) Cobble (1964); (e) Fleming and Crerar (1982); (f) Parkhurst et al. (1980); (g) McGee and Hostetler (1973); (h) Siebert and Hostetler (1977a); (i) Siebert and Hostetler (1977b); (j) Helgeson (1969); (k) Reed (personal communication, 1986, in data base of MINSOLV from Wolery, personal communication, 1978, in DEQPAK5 data set).
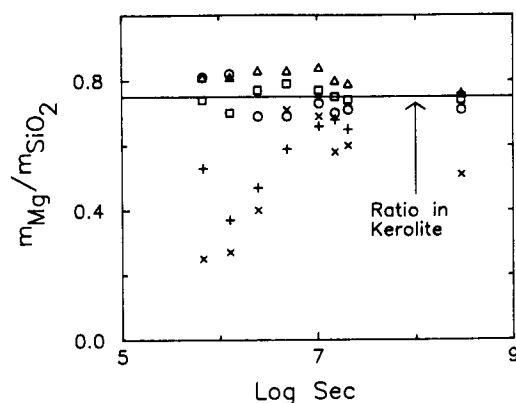

FIG. 4. Aqueous molal ratios of Mg:SiO₂ as a function of reaction time during kerolite hydrolysis in Exp. 6, O; Exp. 7, □; Exp. 8, △; Exp. 9, +; and Exp. 10, ×.

s.d.) for sample set 12 of Exps. 1–5, and 25.79 (±0.24 s.d.) for sample set 9 of Exps. 6–10, respectively. These average values are taken to be the best estimates of the log K values for reactions (1) and (2).

A plot of the final data points from the five sepiolite experiments (sample set 12) and the five kerolite experiments (sample set 9) are plotted as log $(a_{Mg^{2+}}/(a_{H^+})^2)$ versus log $a_{SiO_2(aq)}$ on Fig. 5, a 25°C and 1 bar phase diagram. The size of the rectangles indicate the estimated errors in the activities. The sepiolite and kerolite saturation lines are based on the average log Q values given above as estimates of log K for reactions (1) and (2). No correction was necessary for the decrease in pressure from the experimental conditions of 1 atmosphere to 1 bar. Other saturation lines are based on the thermodynamic data base of HELGESON et al. (1978) for minerals; HELGESON et al. (1974) for water; and HELGESON et al. (1981) for aqueous species.

The five data points of sample set 12 of the sepiolite experiments have a total spread in log Q values of only 0.42 log units. In addition, the estimated log K value of 15.76 agrees within experimental accuracy with the value of 15.86 predicted by CHRIST et al. (1973) from higher temperature dissolution of sepiolite.

The five data points of sample set 9 of the kerolite experiments are less consistent in log Q values than those for the sepiolite experiments. The range in log Q values was 0.62 units in which 4 of the 5 values fall within 0.26 log units. The estimated log K value of 25.79 should be considered a minimum value. Scanning electron microscopy results (see Figs. 1c,d) imply the reacted kerolite may have begun to transform to a more stable phase such as sepiolite. The overall consistency of the five data points in log Q_{ker} is good evidence that dissolution of kerolite is controlling the solution composition. The effect of precipitating minor amounts of another phase will be to lower the measured log Q_{ker} values below the log K_{ker} value.
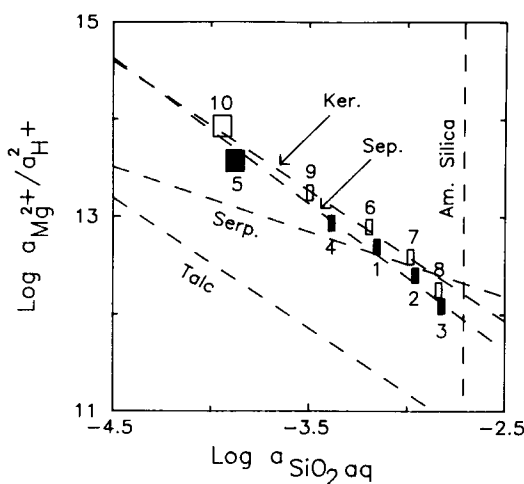

FIG. 5. Final samples from Exps. 1–10 plotted in activity space at 25°C and 1 bar. Note the data from Exps. 6–10 (open rectangles) plot above the data from Exps. 1–5 (shaded rectangles), indicating kerolite is less stable then sepiolite at 25°C. Saturation lines for sepiolite and kerolite are based on log K_{sep} = 15.76 and log K_{ker} = 25.79. Other saturation lines are based on standard state data of HELGESON et al. (1978). Serpentine is based on data for the mineral chrysotile.

25°C and 1 bar molar free energies of formation of sepiolite and kerolite and the change in log K_{sep} between 0 and 100°C

The estimated log K values of reactions (1) and (2) can be used to compute $\Delta \bar{G}^0_{sep,T_r,P_r}$ and $\Delta \bar{G}^0_{ker,T_r,P_r}$, the standard state molar free energies of formation for sepiolite and kerolite at the reference temperature (T_r) of 25°C and the reference pressure (P_r) of 1 bar.

From reactions (1) and (2)

$$\Delta \bar{G}^0_{min,T_r,P_r} = 2.303RT \log K_{min,T_r,P_r} + \sum_i v_i \Delta \bar{G}^0_{i,T_r,P_r};$$

$$= -4,624,340 \text{ J mol}^{-1} \text{ for sepiolite;}$$

$$= -5,736,700 \text{ J mol}^{-1} \text{ for kerolite}$$

where "min" is either sepiolite or kerolite, "i" is a reaction constituent other than the mineral, v_i is the corresponding reaction coefficient, and R and T are the ideal gas constant and temperature in degrees Kelvin, respectively. The standard state molal free energies of formation of water and the aqueous species in the above calculations were taken from HELGESON et al. (1974, Table 29; 1981, Table 18).

Additional molar standard state thermodynamic parameters for sepiolite are needed to compute log K_{sep} as a function of temperature and pressure and to check the 25°C log K_{sep} for consistency with the higher temperature measurements of CHRIST et al. (1973). These are the third law entropy, $\bar{S}^0_{sep,T_r,P_r}$, the volume, $\bar{V}^0_{sep,T_r,P_r}$, and the heat capacity power function coefficients, a_{sep}, b_{sep}, and c_{sep}. The latter are used in Eqn. (5) to compute the heat capacity, $\bar{C}^0_{sep,P_r}$, as

$$\bar{C}^0_{sep,P_r} = a_{sep} + b_{sep}T - c_{sep}T^{-2}. \tag{5}$$

$\bar{V}^0_{sep,T_r,P_r}$ is 142.75 cm^3 mole^{-1}, as calculated from lattice constants given by BRAUNER and PREISINGER (1956, as reported by GRIM, 1968). A structural analogue for sepiolite was used to estimate the heat capacity power coefficients and the third law entropy.

The basic structural units of sepiolite have the formula $Mg_8Si_{12}O_{30}(OH)_4$ with 12 associated water molecules. A projection on the ab plane shows these units to be arranged en echelon with the water molecules in channels (GRIM, 1968, Fig. 4–24). Four of the water molecules are bound to Mg ions and the remainder are "zeolitic" water. Each unit is compositionally equivalent to 3 talc formulas (Mg_9-$Si_{12}O_{30}(OH)_6$) minus one brucite formula ($Mg(OH)_2$) plus 8 "zeolitic" water molecules and four Mg-hydrated water molecules.

From the structural analogue,

$$\bar{S}^0_{sep,T_r,P_r} \simeq \frac{1}{4}(3\bar{S}^0_{talc,T_r,P_r} - \bar{S}^0_{brucite,T_r,P_r}$$

$$+ 8\bar{S}^0_{H_2O \ zeo.,T_r,P_r} + 4\bar{S}^0_{H_2O \ hyd.,T_r,P_r}); \tag{6}$$

and

$$a_{sep} \simeq \frac{1}{4}(3a_{talc} - a_{brucite} + 8a_{H_2O \ zeo.} + 4a_{H_2O \ hyd.}); \tag{7}$$

$$b_{sep} \simeq \frac{1}{4}(3b_{talc} - b_{brucite} + 8b_{H_2O \ zeo.} + 4b_{H_2O \ hyd.}); \tag{8}$$

$$c_{sep} \simeq \frac{1}{4}(3c_{talc} - c_{brucite} + 8c_{H_2O \ zeo.} + 4c_{H_2O \ hyd.}) \tag{9}$$

where Mg-hydrated water was approximated by brucite minus periclase ($Mg(OH)_2 - MgO$). The parameters used in Eqns.

(6)–(9) were taken from the standard state data compilation of HELGESON et al. (1978, Tables 2 and 8). The estimated standard state molar parameters for sepiolite are listed in Table 4.

The apparent standard state free energies of formation for sepiolite, aqueous ions and water have been used to compute log K_{sep} values for reaction (1) at different PT points. The molar third law entropy, molar volume, and the appropriate heat capacity function were used with standard thermodynamic algorithms to move the apparent standard state free energy of formation of sepiolite and the aqueous ions in reaction (1) with temperature. The data in Table 4 were used for sepiolite together with Eqn. (5) for the molar heat capacity. The data in HELGESON et al. (1981) were used with their Eqn. (270) for the aqueous species. The apparent standard state free energy of formation of water was taken from tables (H. C. HELGESON, pers. commun., 1977), as computed from equations and data in HELGESON et al. (1974).

Predicted log K_{sep} values are listed in Table 4 at 5°C intervals between 0° and 100°C at 1 bar and at several PT points of diagenetic interest. The measured log K values from this study and from CHRIST et al. (1973) are plotted on Fig. 6. The predicted curve on Fig. 6 (from Table 4) is consistent with the 51° and 90°C results of CHRIST et al. (1973) but appears inconsistent with their 70°C result as well as the 25°C value from WOLLAST et al. (1968) of 18.78.

DISCUSSION

The study indicates that reaction times on the order of years may be necessary to equilibrate Mg silicates at earth-surface conditions. This is not surprising considering the common absence of such minerals in depositional environments. Aluminum-containing clays are the common authigenic products of the weathering of silicates. These clays prevent the build-up of aqueous Al in solution and consequently act as a sink for silica, and to a lesser extent, for magnesium. Only in areas devoid of unstable Al minerals, will Mg silicates precipitate. These include opal-rich deep sea sediments and carbonate sediments. The former combines a Mg-rich fluid (seawater) with an environment containing an unstable silica
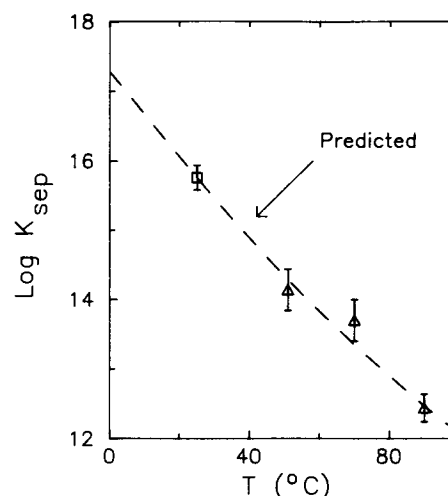

FIG. 6. Predicted log K_{sep} curve between 0° and 100°C and at 1 bar. The experimental data points shown are: 15.76 ± 0.18 at 25°C (this study) and 14.14 ± 0.30 at 51°, 13.70 ± 0.30 at 70° and 12.44 ± 0.20 at 90°C (CHRIST et al., 1973, recalculated for reaction 1).

source (opal). The latter requires a silica-rich fluid which can leach Mg from dolomite or high-Mg calcite.

As shown on Fig. 5, talc will be the stable magnesium silicate at 25°C and 1 bar in contact with natural waters having aqueous SiO_2 concentrations commonly found in natural waters. Serpentine could be stable at very low silica concentrations. Yet these minerals have been rarely reported as forming under earth-surface conditions. Instead, the precipitation rates favor the formation of metastable sepiolite and kerolite in Al-poor environments. The actual difference in solubility between sepiolite and kerolite is small enough that precipitation kinetics probably determine which of these minerals precipitate.

The metastability of kerolite relative to sepiolite, determined in this study, was suggested by JONES (1986). Jones suggests that with increasing pH and aqueous Mg content, and decreasing aqueous SiO_2 content, kerolite will precipitate rather than sepiolite, and that kerolite/stevensite interstratification will occur as aqueous Na content increases. Both sepiolite and kerolite occur as authigenic phases at Amboseli, Kenya, in contact with present-day fluid compositions near amorphous silica saturation and having pH values of around 8 (STOESSELL and HAY, 1978). Kerolite has been reported as a precipitate at Stewart Springs, California, from waters having a pH in excess of 12 (JONES, 1986) but with SiO_2(aq) concentrations below (25°C and 1 bar) quartz saturation. The reported occurrence of kerolite interstratified with stevensite (EBERL et al., 1982) implies kerolite formation is favored during the formation of Al-poor smectites.

The transformation kinetics of dissolution and reprecipitation to talc and serpentine are so slow that sepiolite can be preserved in sediments not exposed to higher temperatures. The apparent beginning of kerolite transformation to a more stable phase, as noted in this study, implies it may not be preserved at low temperatures in older sediments. With increase in temperature (due to burial, hydrothermal activity, or metamorphism) authigenic talc and serpentine are com-

Table 4. Thermodynamic reference data for sepiolite at 25°C and 1 bar and log K_{sep} for reaction (1) at selected PT points.

$\Delta \bar{G}^\circ_{sep}$	$\bar{V}^\circ_{sep}$	$\bar{S}^\circ_{sep}$	a_{sep}	b_{sep} x 10^3	c_{sep} x 10^{-5}
$\frac{J}{mol}$	$\frac{cm^3}{mol}$	$\frac{J}{°K\ mol}$	$\frac{J}{°K\ mol}$	$\frac{J}{mol\ (°K)^2}$	$\frac{J\ °K}{mol}$
-4,624,340.	142.75	335.	389.	134.	54.

bars	°C	log K_{sep}	bars	°C	log K_{sep}
1	0	17.28	1	60	13.83
1	5	16.98	1	65	13.59
1	10	16.67	1	70	13.35
1	15	16.36	1	75	13.12
1	20	16.06	1	80	12.90
1	25	15.76	1	85	12.68
1	30	15.46	1	90	12.47
1	35	15.17	1	95	12.27
1	40	14.89	1	100	12.08
1	45	14.61	2	125	11.19
1	50	14.34	5	150	10.45
1	55	14.08	9	175	9.80
			16	200	9.23
150	60	13.96	500	150	10.88
300	100	12.34	1000	150	11.23
500	100	12.50	500	175	10.24
1000	100	12.85	1000	175	10.61
500	125	11.62	500	200	9.70
1000	125	11.97	1000	200	10.08

mon minerals, forming as direct precipitates or as alteration products of minerals such as sepiolite and kerolite.

The disagreement of the 25°C measured log K_{sep} from this study and that of WOLLAST et al. (1968) is probably due to the lack of equilibrium between their precipitate and seawater. The precipitate had not yet crystallized enough to produce the diagnostic 12 Å peak on an X-ray powder diffraction pattern. They do not report the time intervals over which the solution compositions were monitored in the presence of the precipitate. However, COUTURE (1977) reported the solubility of a sepiolite precipitate was continuing to decrease after 1.3 years. With increasing years of reaction time, the solubility of the precipitate of WOLLAST et al. (1968) should approach that predicted from this study.

On Fig. 6, the 70°C measurement of log K_{sep} by CHRIST et al. (1973) appears to be inconsistent with the predicted curve from this study. The predicted value on Fig. 6, 13.35, is 0.35 log units less positive than their reported experimental (recalculated for reaction 1) value of 13.7 ± 0.3. The 70°C measurement also appears inconsistent with their 51° and 90°C measurements. A sinuous curve would be required to fit those three data points over a temperature interval of 40°, suggesting that the 70°C experimental value may be in error.

REFERENCES

BRADLEY, W. H. (1930) The occurrence and origin of analcite and meerschaum beds in the Green River Formation of Colorado, Wyoming and Utah. U.S. Geol. Surv. Prof. Paper 158, 1–8.

BRAUNER K. and PREISINGER A. (1956) Struktur und Entstehung des Sepiolites. Tschermaks Mineralog. Petrog. Mitt. 6, 120–140.

BRINDLEY G. W. (1959) X-ray and electron diffraction data for sepiolite. Amer. Mineral. 44, 495–500.

BRINDLEY G. W., BISH D. L. and WAN H. M. (1977) The nature of kerolite, its relations to talc and stevensite. Mineral. Mag. 41, 443–452.

CHRIST C. L., HOSTETLER P. B. and SIEBERT R. M. (1973) Studies in the system MgO-SiO₂-CO₂-H₂O (III): The activity-product constant of sepiolite. Amer. J. Sci. 273, 65–83.

COBBLE J. W. (1964) The thermodynamic properties of high temperature aqueous solutions. VI. Applications of entropy correspondence to thermodynamics and kinetics. J. Amer. Chem. Soc. 86, 5394–5401.

COUTURE R. A. (1977) Synthesis of some clay minerals at 25°C; palygorskite and sepiolite in the oceans. Ph.D. dissertation, Univ. of California at San Diego, 237p.

EBERL D. D., JONES B. F. and KHOURY H. N. (1982) Mixed-layer kerolite/stevensite from the Amargosa Desert, Nevada. Clays and Clay Minerals 30, 321–326.

FLEMING B. A. and CRERAR D. A. (1982) Silicic acid ionization and calculation of silica solubility at elevated temperature and pH ap-

plication to geothermal fluid processing and reinjection. Geothermics 11, 15–29.

GRIM R. E. (1968) Clay Mineralogy. McGraw-Hill, New York, 596p.

HATHAWAY J. C. and SACHS P. L. (1965) Sepiolite and clinoptilolite from the Mid-Atlantic Ridge. Amer. Mineral. 50, 852–867.

HAY R. L. and STOESSELL R. K. (1984) Sepiolite in the Amboseli Basin of Kenya: A new interpretation. In Palygorskite-Sepiolite Occurrences, Genesis and Uses (eds. A. SINGER and E. GALAN), Developments in Sedimentology 37, pp. 125–136. Elsevier, New York.

HELGESON H. C. (1969) Thermodynamics of hydrothermal systems at elevated temperatures and pressures. Amer. J. Sci. 167, 729–804.

HELGESON H. C., DELANEY J. M., NESBITT H. W. and BIRD D. K. (1978) Summary and critique of the thermodynamic properties of rock-forming minerals. Amer. J. Sci. 278A, 229.

HELGESON H. C. and KIRKHAM D. M. (1974) Theoretical prediction of the thermodynamic behavior of aqueous electrolytes at high pressures and temperatures: I. Summary of the thermodynamic/electrostatic properties of the solvent. Amer. J. Sci. 274, 1089–1198.

HELGESON H. C., KIRKHAM D. M. and FLOWERS G. C. (1981) Theoretical prediction of the thermodynamic behavior of aqueous electrolytes at high pressures and temperatures: IV. Calculation of activity coefficients, osmotic coefficients, and apparent molal and standard and relative partial molal properties to 600°C and 5 kb. Amer. J. Sci. 281, 1249–1516.

JONES B. F. (1986) Clay mineral diagenesis in lacustrine sediments. U.S. Geol. Surv. Bull. 1578 (in press).

KAUFMAN A. J. (1943) Fibrous sepiolite from Yavapai County, Arizona. Amer. Mineral. 28, 512–520.

KHOURY H. N., EBERL D. D. and JONES B. F. (1982) Origin of magnesium clays from the Amargosa Desert, Nevada. Clays Clay Minerals 30, 327–336.

LIETZKE M. H. and STOUGHTON R. W. (1975) The prediction of osmotic and activity coefficients for electrolyte mixtures at elevated temperatures. Oak Ridge National Laboratory Rept. No. 4999.

MAKSIMOVIC Z. (1966) β-kerolite-pimelite series from Goles Mountain, Yugoslavia. Proc. Intl. Clay Conf. Jerusalem 1, 97–105.

McGEE K. A. and HOSTETLER P. B. (1973) Stability constants for MgOH⁺ and brucite below 100°C. Amer. Geophys. Union Trans. 54, 487.

MULLIN J. B. and RILEY J. P. (1955) The colorimetric determination of silicate with special reference to sea and natural waters. Anal. Chim. Acta 12, 162–176.

PAPKE K. G. (1972). A sepiolite-rich playa deposit in southern Nevada. Clays Clay Minerals 20, 211–215.

PARKHURST D. L., THORSTENSON D. C. and PLUMMER L. N. (1980) PHREEQE—A computer program for geochemical calculations. U.S. Geol. Surv. Water Res. Invest. 80-96. NTIS PB-81 167 801, 210p.

PARRY W. T. and REEVES C. C. JR. (1968) Sepiolite from pluvial Mound Lake, Lynn and Terry Counties, Texas. Amer. Mineral. 53, 984–993.

PLUMMER L. N. and BUSENBERG E. (1982) The solubilities of calcite, aragonite and vaterite in CO₂-H₂O solutions between 0 and 90°C, and an evaluation of the aqueous model for the system CaCO₃-CO₂-H₂O. Geochim. Cosmochim. Acta 46, 1011–1040.

REED M. H. (1982) Calculation of multicomponent chemical equilibria and reaction processes involving minerals, gases and an aqueous phase. Geochim. Cosmochim. Acta 46, 513–528.

ROBINSON R. A. (1936) The dissociation constant of hydrochloric acid. Faraday Soc. Trans. 32, 743–744.

SHAPIRO L. and BRANNOCK W. W. (1962) Rapid analysis of silicate, carbonate, phosphate rocks. U.S. Geol. Surv. Bull. 1144-A, 55p.

SIFFERT B. (1962) Some reactions of silica in solution: Formation of clay. Repts. Geol. Map Service Alsace-Lorraine 21, 100p.

SIEBERT R. M. and HOSTETLER P. B. (1977a) The stability of the magnesium bicarbonate ion pair from 10° to 90°C. Amer. J. Sci. 277, 697–715.

SIEBERT R. M. and HOSTETLER P. B. (1977b) The stability of the magnesium carbonate ion pair from 10° to 90°C. Amer. J. Sci. 277, 716–734.

STOESSELL R. K. (1977) Geochemical studies of two magnesium silicates, sepiolite and kerolite. Ph.D. dissertation, Univ. of California at Berkeley, 122p.

STOESSELL R. K. and HAY R. L. (1978) The geochemical origin of sepiolite and kerolite at Amboseli, Kenya. *Contrib. Mineral. Petrol.* 65, 255–267.

VANDEN HEUVEL R. C. (1966) The occurrence of sepiolite and attapulgite in the calcareous zone of a soil near Las Cruces, New Mexico. *Clays Clay Minerals* 13, 193–207.

WOLLAST R., MACKENZIE F. T. and BRICKER O. P. (1968) Experimental precipitation and genesis of sepiolite at earth-surface conditions. *Amer. Mineral.* 53, 1645–1662.

APPENDIX I

Stoessell (1988) aqueous data from sepiolite hydrolysis experiments at 25°C.

Exp.-sample	Time log(sec)	pH ±0.02	SiO_2 ±2%	Mg^{2+} ±2%	Ca^{2+} ±3%	Na^+ ±5%	K^+ ±5%	eq. x 10⁴ alkalinity ±0.5	log f_{CO_2} calc.	$\frac{m_{Mg}^{2+}}{m_{SiO_2}}$	log Q_{sep}
			total molalities x 10⁴								
1-1	4.32	9.00	0.64	1.70	0.05	0.50	n.m.	1.6	-5.10	2.66	15.54
1-2	4.92	8.90	0.89	1.61	0.06	0.62	n.m.	2.4	-4.79	1.81	15.57
1-3	5.712	6.70	1.27	1.14	0.07	0.71	n.m.	3.0	-4.46	0.90	15.01
1-4	6.120	8.19	1.78	0.56	0.09	0.69	n.m.	2.9	-3.94	0.31	12.89
1-5	6.401	8.08	2.47	0.86	0.12	0.65	n.m.	3.8	-3.71	0.35	13.24
1-6	6.694	7.95	3.16	1.50	0.19	0.69	n.m.	5.1	-3.45	0.47	13.52
1-7	6.984	7.78	5.45	2.92	0.16	0.69	n.m.	7.3	-3.12	0.54	14.11
1-8	7.2949	7.97	5.91	3.46	0.22	0.68	1.84	8.7	-3.24	0.59	15.10
1-9	7.4590	7.72	7.01	4.41	0.20	0.63	2.76	10.3	-2.92	0.63	14.52
1-10	7.5257	7.80	7.15	4.43	0.23	0.60	2.98	10.6	-2.99	0.62	14.87
1-11	7.5910	7.81	7.23	4.51	0.20	0.57	3.14	10.5	-3.00	0.62	14.93
1-12*	8.49843	8.06	7.17	4.59	0.17	0.49	3.27	9.6	-3.29	0.64	15.93
2-1	4.32	3.55	1.25	4.05	0.32	0.73	n.m.	0.0	n.c.	3.24	-4.46
2-2	4.92	4.50	3.71	5.82	0.33	0.73	n.m.	0.0	n.c.	1.57	1.07
2-3	5.712	6.68	7.73	5.36	0.30	0.70	n.m.	1.1	-2.86	0.69	10.68
2-4	6.120	7.29	8.21	5.51	0.26	0.67	n.m.	2.1	-3.18	0.67	13.21
2-5	6.401	7.44	8.72	5.94	0.27	0.67	n.m.	2.3	-3.29	0.68	13.95
2-6	6.694	7.53	9.35	6.17	0.29	0.73	n.m.	2.4	-3.36	0.66	14.43
2-7	6.984	7.49	10.90	7.38	0.24	0.72	n.m.	4.0	-3.10	0.68	14.61
2-8	7.2949	7.66	11.02	7.66	0.29	0.69	2.26	4.4	-3.24	0.70	15.32
2-9	7.4590	7.45	11.47	8.49	0.27	0.63	2.87	5.7	-2.92	0.74	14.62
2-10	7.5257	7.53	11.30	8.23	0.27	0.57	3.14	6.1	-2.96	0.73	14.89
2-11	7.5910	7.51	11.15	7.64	0.26	0.59	3.09	6.1	-2.94	0.69	14.73
2-12*	8.49843	7.79	11.15	8.38	0.09	0.48	2.35	5.6	-3.27	0.75	15.93
3-1	4.30	2.95	1.03	4.80	0.33	0.78	n.m.	0.0	n.c.	4.66	-7.00
3-2	4.92	3.25	3.75	8.57	0.41	0.78	n.m.	0.0	n.c.	2.28	-3.63
3-3	5.712	5.75	12.71	10.77	0.35	0.76	n.m.	0.2	-2.66	0.85	8.16
3-4	6.120	6.93	13.94	11.25	0.30	0.74	n.m.	1.1	-3.11	0.81	13.03
3-5	6.401	7.20	15.17	11.62	0.32	0.72	n.m.	1.6	-3.22	0.77	14.24
3-6	6.694	7.23	15.37	11.31	0.32	0.69	n.m.	1.8	-3.20	0.74	14.36
3-7	6.984	7.23	17.68	13.18	0.26	0.71	n.m.	2.8	-3.01	0.75	14.66
3-8	7.2949	7.43	17.64	13.24	0.32	0.69	1.98	3.4	-3.13	0.75	15.45
3-9	7.4590	7.23	16.95	14.09	0.29	0.66	3.70	3.5	-2.91	0.83	14.64
3-10	7.5257	7.31	17.05	13.65	0.30	0.64	4.19	3.8	-2.95	0.80	14.94
3-11	7.5910	7.28	15.97	12.46	0.28	0.63	4.05	3.9	-2.91	0.78	14.67
3-12*	8.49843	7.57	15.15	11.55	0.09	0.59	3.73	3.3	-3.28	0.76	15.70
4-1	4.36	10.35	0.58	0.96	0.04	18.3	n.m.	21.2	-5.86	1.66	17.80
4-2	4.92	10.05	0.79	2.76	0.06	18.3	n.m.	21.0	-5.36	3.49	18.71
4-3	5.718	9.60	1.02	0.28	0.06	18.3	n.m.	21.0	-4.67	0.27	16.16
4-4	6.122	8.78	1.41	0.26	0.06	18.0	n.m.	21.2	-3.69	0.18	14.01
4-5	6.403	8.60	1.81	0.53	0.11	18.0	n.m.	22.2	-3.48	0.29	14.29
4-6	6.694	8.54	2.23	0.73	0.15	18.9	n.m.	22.2	-3.42	0.33	14.60
4-7	6.984	8.31	3.32	1.51	0.13	20.8	n.m.	24.6	-3.14	0.45	14.88
4-8	7.2949	8.42	3.70	1.62	0.18	21.4	1.43	25.0	-3.25	0.44	15.49
4-9	7.4590	8.15	4.24	2.17	0.18	21.2	3.09	26.5	-2.95	0.51	14.87
4-10	7.5257	8.19	4.39	2.11	0.18	20.8	3.47	26.0	-2.99	0.48	15.05
4-11	7.5910	8.19	4.50	2.30	0.20	19.1	3.46	25.2	-3.01	0.51	15.16
4-12*	8.49843	8.37	4.32	2.06	0.08	17.6	3.15	22.2	-3.25	0.48	15.72
5-1	4.27	10.96	1.55	0.27	0.25	194.	n.m.	198.0	-6.18	0.17	17.31
5-2	4.91	10.81	1.81	0.36	0.25	194.	n.m.	193.4	-5.89	0.20	17.72
5-3	5.717	10.58	2.00	0.20	0.23	194.	n.m.	194.6	-5.44	0.10	17.19
5-4	6.122	10.30	2.29	0.14	0.20	191.	n.m.	196.9	-4.92	0.06	16.79
5-5	6.402	9.96	2.31	0.16	0.17	188.	n.m.	198.7	-4.33	0.07	16.49
5-6	6.694	9.66	1.60	0.21	0.19	195.	n.m.	198.3	-3.87	0.13	15.76
5-7	6.984	9.16	1.91	0.48	0.13	202.	n.m.	203.0	-3.20	0.25	15.54
5-8	7.2949	9.20	2.06	0.50	0.22	211.	2.02	208.3	-3.24	0.24	15.78
5-9	7.4590	9.00	2.23	0.58	0.14	211.	2.74	208.0	-3.00	0.26	15.44
5-10	7.5257	9.02	2.16	0.58	0.16	201.	3.44	200.5	-3.04	0.27	15.48
5-11	7.5910	9.05	2.28	0.59	0.17	191.	3.04	187.6	-3.10	0.26	15.68
5-12*	8.47843	9.20	1.80	0.40	0.09	158.	2.26	167.9	-3.32	0.22	15.51

n.m. not measured; n.c., not calculated because alkalinity was zero.
* Samples used to estimate log K$_{sep}$. Note that decreases in Na concentrations and alkalinity in sample set 12 reflect replacement of fluid taken in sample set 11 with distilled-deionized water.

APPENDIX II

Stoessell (1988) aqueous data from kerolite hydrolysis experiments at 25°C.

Exp.-sample	Time log(sec)	pH	\multicolumn{5}{c}{total molalities x 10^4}	eq. x 10^4 alkalinity	log f_{CO_2} calc.	$\frac{m_{Mg^{2+}}}{m_{SiO_2}}$	log Q_{ker}
			SiO_2	Mg^{2+}	Ca^{2+}	Na^+	K^+				
		±0.02	±2%	±2%	±3%	±5%	±5%	±0.5			
6-1	4.76	9.30	0.33	0.37	0.09	0.25	0.05	1.8	-5.38	1.12	23.86
6-2	5.828	9.15	0.88	0.71	0.28	0.31	0.09	4.3	-4.81	0.81	25.61
6-3	6.106	8.95	1.18	0.97	0.43	0.40	0.49	3.8	-4.64	0.82	25.49
6-4	6.393	8.29	1.91	1.32	0.68	0.40	0.92	6.1	-3.72	0.69	22.97
6-5	6.689	8.06	3.44	2.39	0.90	0.26	1.38	9.1	-3.31	0.69	23.38
6-6#	7.0151	7.80	5.56	4.04	1.10	0.28	1.50	11.7	-2.94	0.73	23.32
6-7	7.1799	7.84	6.08	4.27	1.09	0.29	1.57	11.7	-2.98	0.70	23.78
6-8	7.3133	7.89	6.34	4.49	1.08	0.28	1.88	12.8	-3.00	0.71	24.21
6-9*	8.47227	8.16	6.58	4.70	1.11	0.34	1.98	12.1	-3.30	0.71	25.92
7-1	4.76	6.85	3.12	4.63	1.19	0.25	0.07	1.6	-2.86	1.48	16.83
7-2	5.826	7.73	6.44	4.79	1.24	0.38	0.24	1.8	-3.69	0.74	23.38
7-3	6.109	7.76	6.91	4.85	1.28	0.38	1.19	1.8	-3.72	0.70	23.69
7-4	6.393	7.53	7.22	5.57	1.38	0.39	1.61	3.2	-3.24	0.77	22.56
7-5	6.689	7.62	8.03	6.35	1.26	0.28	1.79	4.7	-3.16	0.79	23.44
7-6#	7.0151	7.51	9.74	7.51	1.29	0.31	1.97	6.7	-2.90	0.77	23.32
7-7	7.1799	7.55	10.05	7.58	1.28	0.31	2.05	6.7	-2.94	0.75	23.62
7-8	7.3133	7.64	10.16	7.47	1.19	0.28	2.30	6.6	-3.04	0.74	24.16
7-9*	8.47227	7.90	10.57	7.84	0.58	0.34	2.21	7.0	-3.28	0.74	25.84
8-1	4.76	3.40	2.87	7.57	1.45	0.25	0.15	0.0	n.c.	2.64	-3.45
8-2	5.828	7.25	12.95	10.46	1.43	0.30	0.15	0.9	-3.51	0.81	22.66
8-3	6.109	7.36	13.01	10.57	1.52	0.33	1.06	1.5	-3.41	0.81	23.33
8-4	6.393	7.26	13.51	11.23	1.52	0.31	1.65	1.7	-3.25	0.83	22.87
8-5	6.689	7.38	14.40	11.96	1.45	0.23	1.79	2.3	-3.25	0.83	23.77
8-6#	7.0151	7.29	15.60	13.10	1.41	0.28	2.02	4.0	-2.91	0.84	23.47
8-7	7.1799	7.32	16.01	12.88	1.44	0.22	2.14	4.6	-2.88	0.80	23.68
8-8	7.3133	7.40	15.54	12.27	1.28	0.28	2.56	4.3	-2.99	0.79	24.05
8-9*	8.47227	7.66	14.65	11.14	0.54	0.26	2.22	4.1	-3.28	0.76	25.40
9-1	4.77	10.40	0.37	0.20	0.07	19.3	0.08	20.1	-5.96	0.54	26.51
9-2	5.829	9.74	0.72	0.38	0.11	19.2	0.13	21.4	-4.85	0.53	26.66
9-3	6.106	9.40	0.97	0.36	0.21	19.1	0.41	22.1	-4.38	0.37	25.78
9-4	6.393	8.72	1.56	0.73	0.36	19.0	0.74	23.4	-3.59	0.47	24.13
9-5	6.689	8.42	2.65	1.57	0.55	20.3	0.96	25.5	-3.24	0.59	24.34
9-6#	7.0151	8.19	3.97	2.61	0.78	20.7	1.16	28.6	-2.95	0.66	24.35
9-7	7.1799	8.20	4.14	2.82	0.85	20.4	1.24	28.8	-2.96	0.68	24.58
9-8	7.3133	8.29	4.37	2.82	0.85	19.9	1.25	28.1	-3.07	0.65	25.20
9-9*	8.47227	8.48	3.39	2.56	0.81	17.6	1.36	25.9	-3.33	0.76	25.76
10-1	4.78	10.95	1.66	0.19	0.64	196.	0.18	195.9	-6.16	0.11	28.28
10-2	5.829	10.56	1.19	0.30	0.37	198.	0.22	197.6	-5.40	0.25	27.73
10-3	6.106	10.33	1.13	0.31	0.36	197.	0.59	198.6	-4.97	0.27	27.26
10-4	6.394	9.86	1.28	0.51	0.34	201.	0.65	199.3	-4.17	0.40	27.04
10-5	6.689	9.28	1.20	0.85	0.20	207.	0.76	205.7	-3.34	0.71	25.66
10-6#	7.0151	9.00	2.06	1.42	0.24	211.	0.78	205.7	-3.01	0.69	26.07
10-7	7.1799	9.03	2.30	1.34	0.26	208.	1.00	206.2	-3.04	0.58	26.32
10-8	7.3133	9.09	2.13	1.27	0.26	206.	0.99	200.5	-3.12	0.60	26.41
10-9*	8.47227	9.24	1.59	0.81	0.13	177.	1.28	184.9	-3.33	0.51	26.02

n.m. not measured; n.c., not calculated because alkalinity was zero.
Successive sample sets in Exps. 6-10 and Exps. 1-5 were taken on the same date beginning with sample set 6 in Exps. 6-10 and sample set 9 in Exps. 1-5.
* Samples used to estimate log K_{ker}. Note that decreases in Na concentrations and alkalinity in sample set 9 reflect replacement of fluid taken in sample set 8 with distilled-deionized water.